Enhancement of the Enzymatic Activity of Ribonuclease HI from *Thermus thermophilus* HB8 with a Suppressor Mutation Method†

Nobutaka Hirano, Mitsuru Haruki, Masaaki Morikawa, and Shigenori Kanaya*

Department of Material and Life Science, Graduate School of Engineering, Osaka University, 2-1 Yamadaoka, Suita, Osaka 565-0871, Japan

Received June 30, 2000; Revised Manuscript Received August 16, 2000

ABSTRACT: A genetic method for isolating a mutant enzyme of ribonuclease HI (RNase HI) from *Thermus thermophilus* HB8 with enhanced activity at moderate temperatures was developed. *T. thermophilus* RNase HI has an ability to complement the RNase H-dependent temperature-sensitive (ts) growth phenotype of *Escherichia coli* MIC3001. However, this complementation ability was greatly reduced by replacing Asp^{134}, which is one of the active site residues, with His, probably due to a reduction in the catalytic activity. Random mutagenesis of the gene encoding the resultant D134H enzyme, followed by screening for second-site revertants, allowed us to isolate three single mutations ($Ala^{12} \rightarrow Ser$, $Lys^{75} \rightarrow Met$, and $Ala^{77} \rightarrow Pro$) that restore the normal complementation ability to the D134H enzyme. These mutations were individually or simultaneously introduced into the wild-type enzyme, and the kinetic parameters of the resultant mutant enzymes for the hydrolysis of a DNA−RNA−DNA/DNA substrate were determined at 30 °C. Each mutation increased the k_{cat}/K_m value of the wild-type enzyme by 2.1−4.8-fold. The effects of the mutations on the enzymatic activity were roughly cumulative, and the combination of these three mutations increased the k_{cat}/K_m value of the wild-type enzyme by 40-fold (5.5-fold in k_{cat}). Measurement of thermal stability of the mutant enzymes with circular dichroism spectroscopy in the presence of 1 M guanidine hydrochloride and 1 mM dithiothreitol showed that the T_m value of the triple mutant enzyme, in which all three mutations were combined, was comparable to that of the wild-type enzyme (75.0 vs 77.4 °C). These results demonstrate that the activity of a thermophilic enzyme can be improved without a cost of protein stability.

Enzymes from thermophilic organisms are generally more stable but less active than their mesophilic counterparts at moderate temperatures, despite the strong resemblance in their structures and functions (*1*−*3*). Comparative studies on hydrogen−deuterium exchange of thermophilic and mesophilic enzymes (*4*), as well as those on dynamic motion (*5*), have suggested that reduction in the conformational flexibility is responsible for the hyperstability and poor enzymatic activity at moderate temperatures of thermophilic enzymes. Introductions of a series of the amino acid substitutions around the active site of barnase (*6*), T4 lysozyme (*7*), and thermolysin (*8*) have also shown that the protein stability increased in proportion to the decrease in the enzymatic activity. However, in vitro evolution studies have recently shown that the activity and stability of enzymes are not correlated with each other (*9*−*13*). Thus, it is controversial as to whether thermophilic enzymes acquire hyperstability at the cost of enzymatic activity.

In vitro evolution (directed evolution) is an efficient technique for engineering protein variants with altered functions. This technique has also been used to probe the relationships between the stability and activity of enzymes. By using this method, the stability of *Bacillus subtilis* esterase was increased by 14 °C in T_m, without any reduction in enzymatic activity at moderate temperatures (*9*). Likewise, the enzymatic activities of *B. subtilis* subtilisin E (*10*) and horse heart myoglobin (*11*) were increased by 256-fold in k_{cat}/K_m and 24.7-fold in k_1 (rate constant for H_2O_2 oxidation of metmyoglobin) without any reduction in protein stability. In addition, mutant enzymes of *B. subtilis* subtilisin E (*12*) and *Bacillus stearothermophilus* catalase I (*13*), in which both the activities and stabilities were increased, have been isolated. These results suggest that enzymes from mesophiles and moderate thermophiles are not optimized with respect to activity and stability. However, it remains to be determined whether this hypothesis is valid for the enzymes from extreme thermophiles. In fact, in vitro evolution of hyperthermostable indoleglyceryl phosphate synthase from an extreme thermophile *Sulfolobus solfataricus* generated mutant enzymes, which are more active at low temperatures but less stable than the wild-type enzyme (*14*). To gain more information about the activity−stability relationships of hyperthermostable enzymes, we used a similar technique to isolate mutant enzymes of *Thermus thermophilus* RNase HI[1] with enhanced activity at moderate temperatures.

T. thermophilus RNase HI, which specifically hydrolyzes the RNA strand of RNA−DNA hybrids, is composed of 166 amino acid residues and acts as a monomer (*1*, *15*). The enzyme had been simply designated as RNase H, until

† This work was supported in part by a Grant-in-Aid for Scientific Research on Priority Areas (A) (12019243) from The Ministry of Education, Science, Sports and Culture of Japan.

* To whom correspondence should be addressed. Telephone or fax: +81-6-6879-7938. E-mail: kanaya@ap.chem.eng.osaka-u.ac.jp.

[1] Abbreviations: GdnHCl, guanidine hydrochloride; DTT, dithiothreitol; CD, circular dichroism; PCR, polymerase chain reaction; RNase HI, ribonuclease HI.

10.1021/bi0015008 CCC: $19.00
Published on Web 10/04/2000

RNases H were classified into two families (type 1 and type 2 RNases H) (*16*). *T. thermophilus* RNase HI is a type 1 enzyme whose amino acid sequence is 52% identical to that of *E. coli* RNase HI, which has been most extensively studied for structures and functions among various RNase H enzymes (*17*−*19*). The three-dimensional structure of *T. thermophilus* RNase HI (*20*) highly resembled that of *E. coli* RNase HI (*21*−*23*). In addition, all the active site residues are conserved and positioned similarly in these two structures, suggesting that *T. thermophilus* RNase HI is indistinguishable from *E. coli* RNase HI in the enzymatic functions, except for protein stability. The former is more stable than the latter by 33.9 °C in T_m at pH 5.5 in the presence of 1.2 M GdnHCl and by 11.8 kcal/mol in ΔG at 25 °C and 14.1 kcal/mol in ΔG at 50 °C (*1*).

To isolate mutant enzymes of *T. thermophilus* RNase HI with enhanced activity generated by random mutagenesis, an appropriate selection system is required. Because a system to determine the RNase H activity by an in situ assay is not available, we decided to develop a genetic system. *E. coli* strain MIC3001 with the *rnh*-339::cat and *rec*B270(Ts) mutations, which shows an RNase H-dependent temperature-sensitive (ts) growth phenotype (*24*), was used for this purpose. This strain would be effective to screen for functional RNase HI mutants in vivo, because the structural genes of type 1 RNases H from *T. thermophilus* HB8 (*15*), *Saccharomyces cerevisiae* (*25*), *Crithidia fasciculata* (*26*), and *Trypanosoma brucei* (*27*) and type 2 RNases H from *E. coli* (*28*), *Streptococcus pneumoniae* (*29*), and *Pyrococcus kodakaraensis* KOD1 (*30*) were successfully cloned via their ability to complement the ts phenotype of this strain. Because *T. thermophilus* RNase HI efficiently complements the ts phenotype of *E. coli* MIC3001, we need to construct a mutant enzyme first, which cannot or can only poorly complement the ts phenotype of *E. coli* MIC3001 due to a reduction in the enzymatic activity. Screening for second-site revertants would allow us to identify the amino acid substitutions that make this mutant enzyme functional in vivo. These amino acid substitutions are expected to increase the activity of the wild-type enzyme. By using a similar genetic method, we have previously succeeded in identifying a number of mutations that increase the thermal stability of *E. coli* RNase HI (*31*). *E. coli* RNase HI complements the ts phenotype of *E. coli* MIC3001, whereas the truncated protein 142-RNase HI, which lacks the 13 C-terminal residues, cannot complement it due to a great reduction in the stability. Eight of eleven single-amino acid substitutions that make 142-RNase HI functional in vivo enhanced the thermal stability of the wild-type enzyme.

Here we report that the Asp^{134} → His mutation greatly reduced the catalytic activity of *T. thermophilus* RNase HI, and the resultant mutant enzyme D134H could only poorly complement the ts phenotype of *E. coli* MIC3001. Random mutagenesis, followed by screening for second site revertants, allowed us to isolate three single-amino acid substitutions, Ala^{12} → Ser, Lys^{75} → Met, and Ala^{77} → Pro, that increase the catalytic efficiency (k_{cat}/K_m) of *T. thermophilus* RNase HI. Combinations of these mutations cumulatively increased the catalytic efficiency of the enzyme without seriously affecting the stability. These results indicate that the activity of an enzyme from extreme thermophiles is not always inversely correlated with its stability.

EXPERIMENTAL PROCEDURES

Materials. Restriction enzymes and modifying enzymes for recombinant DNA technology were from Takara Shuzo Co., Ltd. Guanidine hydrochloride (GdnHCl) was from ICN Biomedicals Inc. Phosphocellulose (P-11) was from Whatman. [γ-^{32}P]ATP (>5000 Ci/mmol) was obtained from Amersham. *E. coli* RNase HI was previously purified (*32*).

Cells and Plasmids. Plasmid pJAL700T, for the overproduction of *T. thermophilus* RNase HI, was constructed previously (*1*). This plasmid bears the wild-type *rnhA* gene under the control of the bacteriophage λ promoters P_R and P_L, the cI^{ts857} gene, and the bacteriophage fd transcription terminator. *E. coli* MIC3001 [*F*$^-$, *sup*E44, *sup*F58, *lac*Y1 or Δ(*lac*IZY)6, *trp*R55, *gal*K2, *gal*T22, *met*B1, *hsd*R14(r_K^-, m_K^+), *rnh*-339::cat, *rec*B270] was previously constructed (*24*). Competent cells of *E. coli* HB101 [*F*$^-$, *hsd*S20(r_B^-, m_B^+), *rec*A13, *ara*-13, *pro*A2, *lac*Y1, *gal*K2, *rps*L20(Sm^r), *xyl*-5, *mtl*-1, *sup*E44, *leu*B6, *thi*-1] and plasmid pBR322 were from Takara Shuzo Co., Ltd. *E. coli* cells were grown in Luria-Bertani medium (*33*) containing 50 mg/L ampicillin.

Plasmid Construction. Plasmid pBR600, which was used for the complementation assay, was constructed by the following procedures. The *rnhA* gene in plasmid pJAL700T was amplified by PCR using primers 1 and 4 as 5′- and 3′-primers, respectively, and primers 2 and 3 as 3′- and 5′-mutagenic primers, respectively, as described previously for the construction of the mutant *E. coli* RNase HI proteins (*34*). The sequences of these primers are shown in Figure 1. The sequence complementary to the 134th codon, which is represented by NNN in the sequence of primer 2, is CTG for Asp in this case. These sequences were designed to silently eliminate the *Mlu*I site encompassing the sequences encoding Lys^3−Val^5 and silently introduce the unique *Sst*II and *Mlu*I sites encompassing the sequences encoding Pro^1−Arg^2 and Glu^{131}−Val^{133}, respectively. After digestion by *Eco*RI and *Hin*dIII, the PCR fragment was ligated into the *Eco*RI−*Hin*dIII sites of plasmid pBR322 to generate plasmid pBR600. The promoter for the *rnhA* gene in this plasmid remains to be determined. The plasmid pBR600 derivatives, which contain the mutant *rnhA* genes with a series of substitutions at codon 134, were constructed by the same procedures, except that primer 2 with a different sequence was used. The sequence of primer 2 was designed so that the GAC codon for Asp^{134} was changed to CAT for His, GAA for Glu, CAA for Gln, TCC for Ser, ACC for Thr, GTC for Val, ATC for Ile, and CTC for Leu. The mutant enzymes of *T. thermophilus* RNase HI at Asp^{134} are designated as D134X, and the mutant *rnhA* genes encoding these mutant enzymes are designated as *rnhA134X*, where X represents the amino acid residue substituted for Asp^{134}. Plasmid pJAL700TM and its derivatives for the overproduction of *T. thermophilus* RNase HI and its mutants were constructed by replacing the small *Nde*I−*Sal*I fragment of pJAL700T with those of pBR600 (Figure 1).

All the primers were synthesized by Sawady Technology Co., Ltd. PCR was performed in 25 cycles with Perkin-Elmer GeneAmp PCR System 2400, using Vent DNA polymerase from New England Biolabs, Inc. The nucleotide sequences of all the wild-type and mutant *rnhA* genes were determined by the dideoxy chain termination method (*35*).

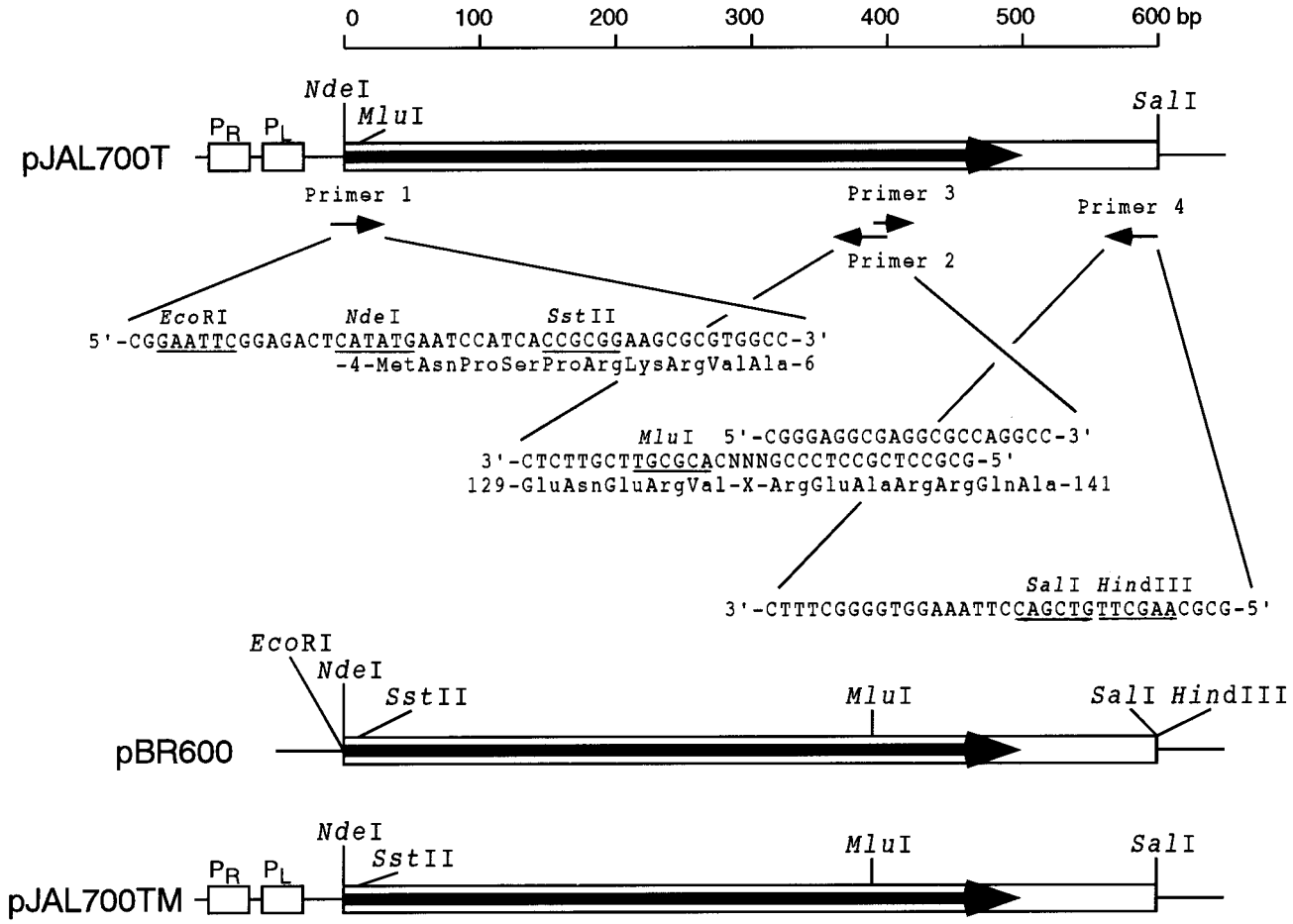

FIGURE 1: Construction of plasmids pBR600 and pJAL700TM. In plasmid pJAL700T, which was used as a template for PCR, the structural gene of *T. thermophilus* RNase HI (large arrow) is under the control of the bacteriophage λ promoters P_R and P_L. Nucleotide sequences together with amino acid sequences of primers 1−4 (small arrows), which were used as 5′- and 3′-mutagenic, 5′-mutagenic, and 3′-primers for PCR, are indicated. Numbers in the amino acid sequences represent the positions of amino acids in the primary structure of *T. thermophilus* RNase HI.

Random Mutagenesis. Random point mutations were introduced into the 5′-terminal 400 bp DNA fragment of the *rnhA* gene by the DNA shuffling method (*36*). This DNA fragment was first amplified from plasmid pBR600 by PCR using primers 1 and 2 (primer 2 with the GAC codon for the 134th residue) (Figure 1). Taq DNA polymerase (Takara Shuzo Co., Ltd.), instead of Vent DNA polymerase, was used for it, because the fidelity of the former is better than that of the latter. This DNA fragment was digested into the 50−100 bp fragments by DNase I in the presence of the Mg^{2+} ion, and then subjected to a primerless PCR using the Taq DNA polymerase to reassemble the DNA fragment. This DNA pool, obtained by the first round of DNA shuffling, was used as a template in PCR with primers 1 and 2. After digestion by *Eco*RI and *Mlu*I, the resultant 400 bp PCR fragment was ligated into the *Eco*RI−*Mlu*I site of plasmid pBR600H, in which the GAC codon for Asp^{134} of the *rnhA* gene was changed to CAT for His. Because this codon is located downstream of the *Mlu*I site (Figure 1), the mutant enzymes screened for second-site revertants always contain the $Asp^{134} \rightarrow$ His mutation, in addition to the mutations introduced by random mutagenesis. We did not carry out the second round of DNA shuffling, because desirable suppressor mutations were introduced into the *rnhA* gene by the first round of DNA shuffling. For the overproduction of the mutant enzymes without the $Asp^{134} \rightarrow$ His mutation, the 400 bp *Nde*I−*Mlu*I fragments of the plasmid pBR600H derivatives were substituted for the corresponding fragment in pJAL700TM. The plasmids for the overproduction of the single-mutant enzymes A12S, K75M, and A77P, in which Ala^{12}, Lys^{75}, and Ala^{77} were replaced with Ser, Met, and Pro, respectively, were designated as pJAL12S, pJAL75M, and pJAL77P, respectively.

Screening for the mutant *rnhA* genes that complemented the ts phenotype of *E. coli* MIC3001 was carried out as described previously (*37*). *E. coli* MIC3001 cells were transformed with the plasmid pBR600H derivatives by electroporation using a Bio-Rad Gene Pulser, as described previously (*38*). The transformants were spread on two Luria-Bertani medium−agar plates with 5 g/L NaCl and 50 mg/L ampicillin, because the ts phenotype of MIC3001 is less pronounced at higher NaCl concentrations (*24*). One was incubated at 42 °C, and the other was incubated at 30 °C. The colonies grown at 42 °C were selected, and the plasmid pBR600H derivatives were isolated from each clone. After it had been confirmed that each plasmid suppressed the ts phenotype of *E. coli* MIC3001, the nucleotide sequences of the mutant *rnhA* genes were determined.

Combinations of Activating Mutations. Plasmid pJAL75M/77P for the overproduction of the double-mutant enzyme K75M/A77P was constructed by site-directed mutagenesis using PCR, as described previously for the construction of

the mutant *E. coli* RNase HI proteins (*34*). Primers 1 and 4 shown in Figure 1 were used as 5′- and 3′-primers, respectively, and appropriate primers, instead of primers 2 and 3, were used as mutagenic primers. These mutagenic primers were designed so that the codon for Lys^{75} was changed from AAG to ATG for Met and the codon for Ala^{77} was changed from GCC to CCC for Pro. pJAL12S, pJAL75M, pJAL77P, and pJAL75M/77P contain the unique *Sac*I site encompassing the sequences encoding Glu^{48}−Leu^{49}. Therefore, plasmids pJAL12S/75M, pJAL12S/77P, and pJAL12S/75M/77P for the overproduction of the double-mutant enzymes A12S/K75M and A12S/A77P and the triple-mutant enzyme A12S/K75M/A77P were constructed by replacing the small *Sac*I−*Sal*I fragment of plasmid pJAL12S with the corresponding fragments of plasmids pJAL75M, pJAL77P, and pJAL75M/77P, respectively.

Overproduction and Purification. The overproducing strains were constructed by transforming *E. coli* HB101 with the plasmid pJAL700TM derivatives. Cultivation of these strains and overproduction and purification of the mutant enzymes were carried out as described previously for the wild-type enzyme (*39*), except that all the purification procedures were carried out in the presence of 1 mM dithiothreitol (DTT). The protein concentration was determined from UV absorption, assuming that all the mutant enzymes obtained in this experiment have the same $A_{280}^{0.1\%}$ value (1.6) as that of the wild-type enzyme (*1*). The production levels of the mutant enzymes and their purities were estimated by subjecting whole cell lysates and purified samples to SDS−PAGE on a 15% polyacrylamide gel (*40*), followed by staining with Coomassie Brilliant Blue.

RNase H Assay. The enzymatic activity was determined in 10 mM Tris-HCl (pH 8.0) containing 10 mM $MgCl_2$, 50 mM NaCl, 1 mM DTT, and 50 μg/mL bovine serum albumin at 30 or 60 °C by using a ^{32}P-labeled 29 bp DNA−RNA−DNA/DNA as a substrate. The 29 b DNA−RNA−DNA (5′-AATAGAGAAAAAGaaaaAAGATGGCAAAG-3′), in which DNA and RNA are represented by uppercase and lowercase letters, respectively, and the 29 b DNA, which is complementary to this 29 b DNA−RNA−DNA, were kindly donated by ID Biomedical Corp. The preparation of the ^{32}P-labeled 29 bp DNA−RNA−DNA/DNA substrate and the quantitative analyses of the products separated with a 20% polyacrylamide gel containing 7 M urea using an Instant Imager from Packard were carried out as described previously (*30*). One unit was defined as the amount of the enzyme producing 1 μmol of products per minute. The specific activity was defined as the enzymatic activity per milligram of protein. For the determination of the kinetic parameters, the concentration of the ^{32}P-labeled 29 bp DNA−RNA−DNA/DNA substrate was varied from 0.2 to 10 μM such that it spanned the K_m value. The amount of the enzyme was controlled carefully such that the fraction of the substrate hydrolyzed did not exceed 30% of the total. Under this condition, the amount of the product increased in proportion to the increase in the amount of the enzyme or the reaction time.

Circular Dichroism Spectra. The CD spectra were recorded on a J-725 automatic spectropolarimeter from Japan Spectroscopic Co., Ltd., at 30 °C in 10 mM sodium acetate (pH 5.5) containing 0.1 M NaCl and 1 mM DTT. For the measurement of the far-ultraviolet (UV) CD spectra (200−260 nm), the protein concentration was approximately 0.13 mg/mL and a cell with an optical path length of 2 mm was used. For the measurement of the near-UV CD spectra (240−320 nm), the protein concentration was 0.5−1.0 mg/mL and a cell with an optical path length of 10 mm was used. The mean residue ellipticity, θ, which has units of deg cm^2 dmol^{-1}, was calculated by using an average amino acid molecular weight of 110.

Thermal Denaturation. The thermal denaturation curves and the temperature of the midpoint of the transition, T_m, were determined as described previously (*41*) by monitoring the change in the CD value at 220 nm. The enzymes were dissolved in 20 mM sodium acetate (pH 5.5) containing 1 M GdnHCl and 1 mM DTT. The protein concentration was approximately 0.13 mg/mL, and a cell with an optical path length of 2 mm was used. The enthalpy change of unfolding at the T_m (ΔH_m) and the entropy change of unfolding at the T_m (ΔS_m) were calculated by van't Hoff analysis. The difference in the free energy change of unfolding between the mutant and wild-type enzymes, at the T_m of the wild-type enzyme ($\Delta\Delta G_m$), was estimated by the relationship given by Becktel and Schellman (*42*) ($\Delta\Delta G_m = \Delta T_m \Delta S_m$). ΔT_m is the change in T_m of a mutant enzyme relative to that of the wild-type enzyme. The ΔS_m value of the wild-type enzyme was determined to be 0.269 kcal mol^{-1} K^{-1} from four independent experiments with errors of ±0.04 kcal mol^{-1} K^{-1}. This value was used for the calculation of the $\Delta\Delta G_m$ values.

RESULTS

Mutations at Asp^{134}. We have previously shown that Asp^{134} of *E. coli* RNase HI is involved in a catalytic function, but nine amino acid residues (Asn, His, Glu, Gln, Ser, Thr, Val, Ile, and Leu) are permissive at this position (*37*). All the resultant mutant enzymes retained the ability to complement the ts phenotype of *E. coli* MIC3001. However, the complementation abilities of these mutant enzymes, which were estimated from the sizes of the colonies of *E. coli* MIC3001 transformants grown at 42 °C, were correlated with the levels of their enzymatic activities. These results prompted us to examine whether the mutations at Asp^{134} of *T. thermophilus* RNase HI equally reduce the catalytic activity of the enzyme and thereby reduce its complementation ability. All the amino acid residues that have been shown to be permissive at position 134 of *E. coli* RNase HI, except for Asn, were substituted for Asp^{134} of *T. thermophilus* RNase HI, and the effects of these mutations on the complementation ability of the enzyme were analyzed. The effect of the $Asp^{134} \rightarrow$ Asn mutation was not analyzed, because the D134N enzyme is expected to retain almost full activity as did the *E. coli* RNase HI variant with this mutation (*43*). Interestingly, all the mutant enzymes, except for the D134H enzyme, in which Asp^{134} was replaced with His, lost the complementation ability, suggesting that these mutant enzymes are not functional in vivo. The D134H enzyme retained a low level of complementation ability, as compared to that of the wild-type enzyme. When *E. coli* MIC3001 transformants with pBR600 and pBR600H, in which the wild-type and D134H enzymes are produced, were grown on the plates at 42 °C for 18 h, the former formed colonies whereas the latter did not. *E. coli* MIC3001 transformants with pBR600H formed colonies only when they were grown at 42 °C for more than

Table 1: Kinetic Parameters of the Wild-Type and Mutant Enzymes[a]

enzyme	K_m (μM)	k_{cat} (min^{-1})	k_{cat}/K_m (μM^{-1} min^{-1})	relative k_{cat}/K_m	hypothetical relative k_{cat}/K_m
wild-type	7.8	4.9	0.63	1.0	1.0
D134H	3.3	0.18	0.055	0.087	
A12S	1.5	4.5	3.0	4.8	
K75M	6.1	8.0	1.3	2.1	
A77P	3.3	7.3	2.2	3.5	
A12S/K75M	1.1	12	11	17	10
A12S/A77P	1.3	15	12	19	17
K75M/A77P	2.0	20	10	16	7.4
A12S/K75M/A77P	1.1	27	25	40	35

[a] The enzymatic activity was determined at 30 °C for 15 min in 10 mM Tris-HCl (pH 8.0) containing 10 mM $MgCl_2$, 50 mM NaCl, 50 μg/mL bovine serum albumin, and 1 mM DTT, by using ^{32}P-labeled 29 bp DNA−RNA−DNA/DNA as a substrate. The kinetic parameters were determined by a least-squares fit of the data obtained from the Lineweaver−Burk plots. The relative k_{cat}/K_m was calculated by dividing the k_{cat}/K_m value of the mutant enzyme by that of the wild-type enzyme. Hypothetical relative k_{cat}/K_m values were calculated by multiplying the relative k_{cat}/K_m values of the single-mutant enzymes with constituent substitutions. Errors are within 30% for the K_m and k_{cat} values reported, which are the averages of two independent experiments.

Table 2: Thermodynamic Parameters of the Wild-Type and Mutant Enzymes[a]

enzyme	T_m (°C)	ΔT_m (°C)	ΔH_m (kcal/mol)	$\Delta\Delta G_m$ (kcal/mol)	hypothetical $\Delta\Delta G_m$ (kcal/mol)[b]
wild-type	77.4		94.3		
D134H	79.4	2.0	101.3	0.54	
A12S	76.0	−1.4	86.7	−0.38	
K75M	78.2	0.8	93.2	0.22	
A77P	71.7	−5.7	77.2	−1.53	
A12S/K75M	76.8	−0.6	103.4	−0.16	−0.16
A12S/A77P	71.0	−6.4	87.3	−1.72	−1.91
K75M/A77P	75.6	−1.8	90.5	−0.48	−1.31
A12S/K75M/A77P	75.0	−2.4	100.5	−0.65	−1.69

[a] Errors are within ±0.5 °C for T_m, ±15 kcal/mol for ΔH_m, and ±0.2 kcal/mol for $\Delta\Delta G_m$. [b] Hypothetical $\Delta\Delta G_m$ values represent the sum of the $\Delta\Delta G_m$ values of the single-mutant enzymes with constituent substitutions.

24 h. We used the D134H enzyme for screening of second-site revertants.

Enzymatic Activity and Thermal Stability of the D134H Enzyme. To confirm that the reduction in the complementation ability of the D134H enzyme is due to the reduction in its catalytic activity, the enzymatic activity and thermal stability of the purified D134H enzyme were determined and compared with those of the wild-type enzyme. The kinetic parameters of the wild-type and D134H enzymes were determined at 30 °C using the 29 bp DNA−RNA−DNA/DNA substrate. This substrate is suitable for determining the kinetic parameters of the RNase HI enzymes, because it is cleaved by *E. coli* RNase HI at a unique position in the middle of the four-adenosine sequence (*30*). *T. thermophilus* RNase HI and its variants constructed in this experiment also cleaved it at this position (data not shown). The results are summarized in Table 1. The Asp^{134} → His mutation resulted in a large reduction in the k_{cat} value, along with a slight reduction in the K_m value. As the result, the catalytic efficiency (k_{cat}/K_m) of the D134H enzyme, which was only ∼9% of that of the wild-type enzyme, was decreased due to the reduction in the hydrolysis rate (k_{cat}).

The thermal denaturation curves of the wild-type and D134H enzymes were measured by monitoring the change in the CD values at 220 nm at pH 5.5 in the presence of 1 M GdnHCl and 1 mM DTT. Both enzymes were shown to unfold reversibly in a single cooperative fashion under this condition (data not shown). The thermodynamic parameters of these enzymes are summarized in Table 2. The T_m value of the wild-type enzyme (77.4 °C) was identical with that determined previously at pH 5.5 in the presence of 1 M GdnHCl and 20 mM 2-mercaptoethanol (*39*), suggesting that the thermal denaturation curve of the wild-type enzyme obtained in this experiment represents that of the enzyme in a reduced form. The D134H enzyme was more stable than the wild-type enzyme by 2.0 °C in T_m and 0.54 kcal/mol in ΔG_m, suggesting that the Asp^{134} → His mutation is not unfavorable for the conformational stability. The far-UV CD spectrum of the D134H enzyme was basically identical with that of the wild-type enzyme, suggesting that the protein conformation was not markedly changed by the mutation.

Screening for Suppressor Mutations. The screening for second-site revertants of a mutant protein often results in the reversion of the original point mutation, rather than yielding true second-site reversions. Therefore, we introduced random mutagenesis into the upstream region of the codon 134 in the *rnhA134H* gene, to avoid the reversion of the original point mutation at codon 134. This region encompasses the sequences encoding amino acid residues at positions 7−128 (Figure 1). When *E. coli* MIC3001 transformants were examined for their growth at 42 °C, the transformants which form colonies in 18 h were obtained with a frequency of 1 in 10^4. Plasmid DNAs were isolated from 10 colonies grown at 42 °C (strains 1−10), and the DNA sequences of the mutant *rnhA134H* genes were determined. The results are summarized in Table 3. Strains 2 and 10 produced the same variant of the D134H enzyme with a single Ala^{77} → Pro mutation. Likewise, strains 5 and 8 produced the D134H enzyme variants with single Lys^{75} → Met and Ala^{12} → Ser mutations, respectively. Other strains produced the D134H enzyme variants with double and quadruple mutations, in which either the Ala^{12} → Ser, Lys^{75} → Met, or Ala^{77} → Pro mutation is always included. The complementation levels of the enzyme variants with double or quadruple mutations were similar to or below those of the enzyme variants with single mutations. These results strongly suggest that, of the 11 mutations isolated in this experiment, only the Ala^{12} → Ser, Lys^{75} → Met, or Ala^{77} → Pro mutation can suppress the effect of the Asp^{134} → His mutation on the complementation ability of the enzyme. To analyze the effects of these mutations on the activity and stability of the wild-type enzyme, the mutant enzymes with these suppressor mutations alone were constructed, purified to give a single band on SDS−PAGE, and characterized for activities and stabilities. We have not purified and biochemically characterized the mutant enzymes with both suppressor and Asp^{134} → His mutations.

Enzymatic Activities of Mutant Enzymes. The kinetic parameters of the mutant enzymes, in which suppressor mutations were individually introduced or combined, were determined at 30 °C using the 29 bp DNA−RNA−DNA/DNA substrate and compared with those of the wild-type enzyme. The results are summarized in Table 1. The Ala^{12}

Table 3: Complementation Levels of the Revertants of the D134H Enzyme and Mutations Contained in These Revertants[a]

strain number	complementation level	mutations with amino acid substitutions	mutations without amino acid substitutions
1	++	Ala^{12} → Ser (G<u>C</u>C → T<u>C</u>C) *Lys^{122} → Arg (A<u>A</u>G → A<u>G</u>G)*	Ala^{52} (GC<u>C</u> → GC<u>T</u>) Val^{116} (GT<u>G</u> → GT<u>A</u>)
2	++	Ala^{77} → Pro (G<u>C</u>C → C<u>C</u>C)	Cys^{13} (TG<u>C</u> → TG<u>T</u>)
3	+	Ala^{12} → Ser (G<u>C</u>C → T<u>C</u>C) *Leu^{35} → Pro (C<u>T</u>C → C<u>C</u>C)* *Ala^{93} → Val (G<u>C</u>G → G<u>T</u>G)* *Arg^{117} → Cys (C<u>G</u>C → T<u>G</u>C)*	Glu^{48} (GA<u>G</u> → GA<u>A</u>)
4	+	Lys^{75} → Met (A<u>A</u>G → A<u>T</u>G) *His^{119} → Tyr (C<u>A</u>C → T<u>A</u>C)*	
5	++	Lys^{75} → Met (A<u>A</u>G → A<u>T</u>G)	Leu^{25} (CT<u>C</u> → CT<u>T</u>)
6	++	*Ala^{40} → Pro (G<u>C</u>C → C<u>C</u>C)* Lys^{75} → Met (A<u>A</u>G → A<u>T</u>G)	Leu^{25} (CT<u>C</u> → CT<u>T</u>) Ala^{93} (GC<u>G</u> → GC<u>A</u>)
7	+	*Glu^{64} → Gly (G<u>A</u>G → G<u>G</u>G)* Ala^{77} → Pro (G<u>C</u>C → C<u>C</u>C)	Leu^{25} (CT<u>C</u> → CT<u>T</u>)
8	++	Ala^{12} → Ser (G<u>C</u>C → T<u>C</u>C)	
9	+	Lys^{75} → Met (A<u>A</u>G → A<u>T</u>G) *Glu^{105} → Gly (G<u>A</u>G → G<u>G</u>G)*	
10	++	Ala^{77} → Pro (G<u>C</u>C → C<u>C</u>C)	Phe^{28} (TT<u>C</u> → TT<u>T</u>)

[a] The complementation level was estimated from the size of the colonies of *E. coli* MIC3001 transformants at 42 °C (++ for large and + for medium sizes). *E. coli* MIC3001 transformants with plasmid pBR600 gave large colonies, whereas those with plasmid pBR600H gave small colonies. The codons with mutations are shown in parentheses, in which underlined residues are the substituted nucleotides. The mutations, which alone may not be able to improve the complementation ability of the D134H enzyme, are shown in italics.

→ Ser mutation decreased the K_m value by 5.2-fold without seriously affecting the k_{cat} value. The Lys^{75} → Met mutation increased the k_{cat} value by 1.6-fold without seriously affecting the K_m value. The Ala^{77} → Pro mutation decreased the K_m value by 2.4-fold and increased the k_{cat} value by 1.5-fold. Accordingly, all of these mutations increased the k_{cat}/K_m value of the wild-type enzyme by 2.1−4.8-fold. These results indicate that all the suppressor mutations, which restored normal complementation ability to the D134H enzyme, enhanced the catalytic efficiency of the wild-type enzyme at moderate temperatures. Combination of these suppressor mutations generated more active mutant enzymes with k_{cat}/K_m values that were higher than that of the wild-type enzyme by 16−40-fold (Table 1). Of them, the A12S/K75M/A77P enzyme, which contains all three suppressor mutations, exhibited the highest catalytic efficiency. The k_{cat}/K_m value of this triple-mutant enzyme was comparable to the hypothetical value, which was calculated assuming that the effect of each suppressor mutation on the enzymatic activity is cumulative. The k_{cat}/K_m values of the A12S/K75M and K75M/A77P enzymes were higher than the hypothetical values, but only by at most 2-fold. Thus, the effect of each suppressor mutation on the enzymatic activity was roughly cumulative.

To examine whether the mutant enzymes with suppressor mutations are more active than the wild-type enzyme at elevated temperatures as well, the specific activities of the wild-type and A12S/K75M/A77P enzymes were determined at 30 and 60 °C using the 29 bp DNA−RNA−DNA/DNA substrate (Table 4). This triple-mutant enzyme was chosen as a representative, because it exhibited the highest activity at 30 °C. The specific activity of this mutant enzyme was higher than that of the wild-type enzyme by ~20-fold at both 30 and 60 °C, suggesting that combination of three suppressor mutations enhanced the enzymatic activity of *T. thermophilus* RNase HI at its optimum temperature. The optimum temperature of *T. thermophilus* RNase HI has not been determined, because the duplex form of the substrate is denatured at temperatures higher than 70 °C.

Table 4: Comparison of Specific Activities of the Wild-Type and A12S/K75M/A77P Enzymes[a]

enzyme	temperature (°C)	specific activity (units/mg)	relative activity
wild-type	30	0.029	1.0
	60	0.78	27
A12S/K75M/A77P	30	0.59	20
	60	15	517

[a] Specific activities were determined at 30 and 60 °C for 15 min by using ^{32}P-labeled 29 bp DNA−RNA−DNA/DNA as a substrate under the conditions described in the footnote of Table 1. The enzymes and substrates were preincubated for 5 min at designated temperatures. One unit was defined as the amount of the enzyme producing 1 μmol of products. The concentration of the substrate was 1 μM. Errors are within 30% for the reported values, which are the averages of two independent experiments.

Thermal Stability. To analyze the effects of the suppressor mutations on the protein stability, the thermal denaturation curves were measured by monitoring the change in the CD values at 220 nm (Figure 2). All mutant enzymes were shown to reversibly unfold in a single cooperative fashion. The thermodynamic parameters of these mutant enzymes, which were obtained by assuming that these enzymes unfold via a two-state mechanism, are summarized in Table 2. Of the single-mutant enzymes, only the A77P enzyme was considerably less stable than the wild-type enzyme by 5.7 °C in T_m and 1.53 kcal/mol in ΔG_m, indicating that the Ala^{77} → Pro mutation considerably decreased the protein stability, whereas other mutations did not seriously affect it. However, the K75M/A77P and A12S/K75M/A77P enzymes, which contain both the Lys^{75} → Met and Ala^{77} → Pro mutations, were less stable than the wild-type enzyme only by 1.8 and 2.4 °C in T_m and 0.48 and 0.65 kcal/mol in ΔG_m, respectively. These results suggest that the destabilization effect of the Ala^{77} → Pro mutation is compensated by the Lys^{75} → Met mutation, which does not seriously affect the protein stability by itself. The Ala^{12} → Ser mutation did not compensate for this destabilization effect, because the A12S/A77P enzyme was less stable than the wild-type enzyme by

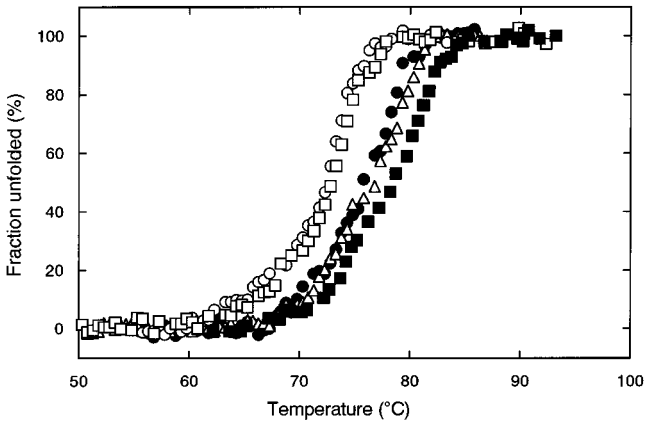

FIGURE 2: Thermal denaturation curves of the wild-type and mutant enzymes. The apparent fraction of unfolded protein is shown as a function of temperature. Thermal denaturation curves of the wild type and all of the mutant enzymes were determined at pH 5.5 in the presence of 1 M GdnHCl and 1 mM DTT by monitoring the change in the CD value at 220 nm, as described in Experimental Procedures. The curves of the wild-type (■), A77P (□), A12S/A77P (○), K75M/A77P (△), and A12S/K75M/A77P (●) enzymes are shown as representatives.

6.4 °C in T_m and 1.72 kcal/mol in ΔG_m. To evaluate the cooperative effects of the Lys[75] → Met and Ala[77] → Pro mutations on the protein stability more quantitatively, the hypothetical $\Delta\Delta G_m$ values were calculated for the multiple-mutant enzymes by simply adding the $\Delta\Delta G_m$ values of the single-mutant enzymes with constituent substitutions (Table 2). The $\Delta\Delta G_m$ values of the A12S/K75M and A12S/A77P enzymes were almost identical with the hypothetical values. In contrast, the $\Delta\Delta G_m$ values of the K75M/A77P and A12S/K75M/A77P enzymes were higher than the hypothetical values by ~1 kcal/mol in ΔG_m.

CD Spectra. The far-UV CD spectra of all mutant enzymes, except for those of the K75M/A77P and A12S/K75M/A77P enzymes, were indistinguishable from that of the wild-type enzyme (data not shown). All spectra gave a broad trough with a minimum [θ] value of approximately −12500 around 210−215 nm. However, the spectra of the K75M/A77P and A12S/K75M/A77P enzymes, which were similar to each other, were different from that of the wild-type enzyme in the 220−235 nm region (Figure 3a). In this region, the former spectra were sharper than the latter spectrum. As a result, the former spectra gave another small minimum with a [θ] value of approximately −2500 at 235 nm, whereas the latter spectrum did not. This difference may be produced by conformational changes of the aromatic residues, because the spectrum of the K75M/A77P or A12S/K75M/A77P enzyme in the 200−220 nm region, which reflects the content of the secondary structures of the protein, is similar to that of the wild-type enzyme, and because a positive contribution of the tryptophan residue to the CD spectrum at 228 nm has been reported (*44*). In fact, the near-UV CD spectra of the K75M/A77P and A12S/K75M/A77P enzymes, which reveal the three-dimensional environments of the aromatic residues, were slightly different from that of the wild-type enzyme (Figure 3b), whereas those of other mutant enzymes were basically the same as that of the wild-type enzyme (data not shown). These results suggest that the simultaneous introduction of the Lys[75] → Met and Ala[77] → Pro mutations causes a local conformational change, but only to a small extent. Thus, all the mutations did not seriously affect the overall structure of the enzyme.

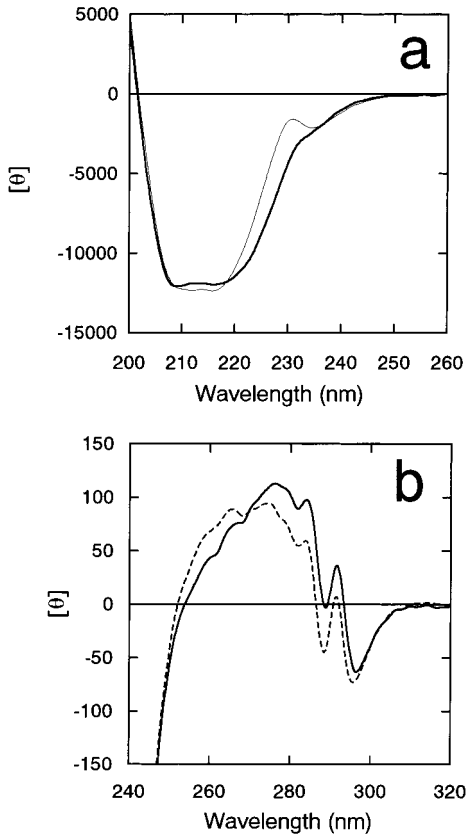

FIGURE 3: CD spectra of the wild-type and mutant enzymes. The CD spectra of the wild type and all mutant enzymes were measured as described in Experimental Procedures. (a) The far-UV CD spectrum of the K75M/A77P enzyme (thin line) is shown in comparison with that of the wild-type enzyme (thick line). The far-UV CD spectrum of the A12S/K75M/A77P enzyme is basically the same as that of the K75M/A77P enzyme. The far-UV CD spectra of all other mutant enzymes are basically the same as that of the wild-type enzyme. (b) The near-UV CD spectrum of the A12S/K75M/A77P enzyme (broken line) is shown in comparison with that of the wild-type enzyme (thick line). The near-UV CD spectrum of the K75M/A77P enzyme is similar to that of the A12S/K75M/A77P enzyme, whereas those of other mutant enzymes are similar to that of the wild-type enzyme.

DISCUSSION

Strategy for Enhancing Enzymatic Activity. In this study, we employed suppressor mutation methods to improve the enzymatic activity of *T. thermophilus* RNase HI. This method includes complementation of the RNase H-dependent ts phenotype of *E. coli* MIC3001. Of the eight mutant enzymes, in which Asp[134] was replaced with various amino acid residues, only the D134H enzyme complemented the ts phenotype of *E. coli* MIC3001, but with poor efficiency. Because the enzymatic activity of the D134H enzyme must be close to the critical level of RNase H activity, which is required to complement the ts phenotype of *E. coli* MIC3001, a slight increase in the enzymatic activity would be sufficient to improve the complementation ability of this mutant enzyme. In fact, screening for the second-site revertants of the D134H enzyme allowed us to isolate three suppressor mutations that improved the catalytic efficiency of the wild-type enzyme by only 2.1−4.8-fold. In contrast, attempts to isolate second-site revertants of other mutant enzymes, such

as D134E and D134Q, have been so far unsuccessful (data not shown). In addition, none of the suppressor mutations of the D134H enzyme were sufficient to make these mutant enzymes functional in vivo, even when all of them were combined (data not shown). Therefore, the enzymatic activities of other mutant enzymes must be lower than the critical level by more than 40-fold. These results are consistent with the previous ones wherein the $Asp^{134} \rightarrow$ His mutation reduced the enzymatic activity of *E. coli* RNase HI by only 40%, whereas other mutations dramatically reduced it by more than 100-fold (*37*). The complementation abilities of the *T. thermophilus* RNase HI variants were always lower than those of the corresponding *E. coli* RNase HI variants, probably because the enzymatic activity of *T. thermophilus* RNase HI in the *E. coli* cells is much lower than that of *E. coli* RNase HI. The specific activity of *T. thermophilus* RNase HI determined under its optimal condition, except for the temperature, has been reported to be lower than that of *E. coli* RNase HI by 5-fold at 30 °C (*1*).

$Ala^{12} \rightarrow Ser$ Mutation. The $Ala^{12} \rightarrow$ Ser mutation improved the affinity of the enzyme for the substrate, without seriously affecting the hydrolysis rate and thermal stability of the enzyme. Ala^{12} is located in the βA strand and exposed to the solvent (Figure 4a). This residue is replaced with Ser in *E. coli* RNase HI. Because other residues around this residue from Phe^{8} to Gly^{21} are fully conserved in *E. coli* RNase HI, the $Ala^{12} \rightarrow$ Ser mutation makes the sequence of a peptide segment from Phe^{8} to Gly^{21} identical with that of *E. coli* RNase HI. Structural and mutational studies of *E. coli* RNase HI revealed that Asp^{10}, Glu^{48}, Asp^{70}, His^{124}, and Asp^{134} form the active site (*19*). According to the latest model for the catalytic mechanism of the enzyme (*45*), His^{124} accepts a proton from an attacking H_2O molecule that acts as a general base. Asp^{134} holds this H_2O molecule. Glu^{48} anchors the H_2O molecule that acts as a general acid. Asp^{10}, as well as the main chain carbonyl oxygen of Gly^{11}, provides coordinating groups for binding of the catalytically essential Mg^{2+} ion. Asp^{70} governs the conformation of Asp^{10}. In addition, a large cleftlike depression, which extends from the negatively charged active site to the positively charged αIII helix and the following loop, has been proposed to form the substrate binding site (*19*). Cys^{13}, Asn^{16}, Thr^{43}, Asn^{44}, and Asn^{45} located in this depression have been shown to be involved in substrate binding (*46*). All of these residues involved in the catalytic function and substrate binding are conserved in *T. thermophilus* RNase HI. Of them, Asp^{10}, Gly^{11}, Cys^{13}, and Asn^{16} are located in a peptide segment from Phe^{8} to Gly^{21}. Therefore, it seems likely that the $Ala^{12} \rightarrow$ Ser mutation causes a conformational change, which is favorable for the amino acid residues involved in substrate binding. This conformational change must be subtle, because the far- and near-UV CD spectra of the A12S enzyme were almost identical with those of the wild-type enzyme. It is unlikely that Ser^{12} of the A12S enzyme forms a hydrogen bond with the substrate and thereby improves the affinity of this mutant enzyme for the substrate, because the substrate titration experiment using NMR previously indicated that Ser^{12} of *E. coli* RNase HI is not directly involved in substrate binding (*46*).

$Lys^{75} \rightarrow Met$ and $Ala^{77} \rightarrow Pro$ Mutations. The $Lys^{75} \rightarrow$ Met mutation increased the hydrolysis rate of the enzyme, without seriously affecting the affinity for the substrate and

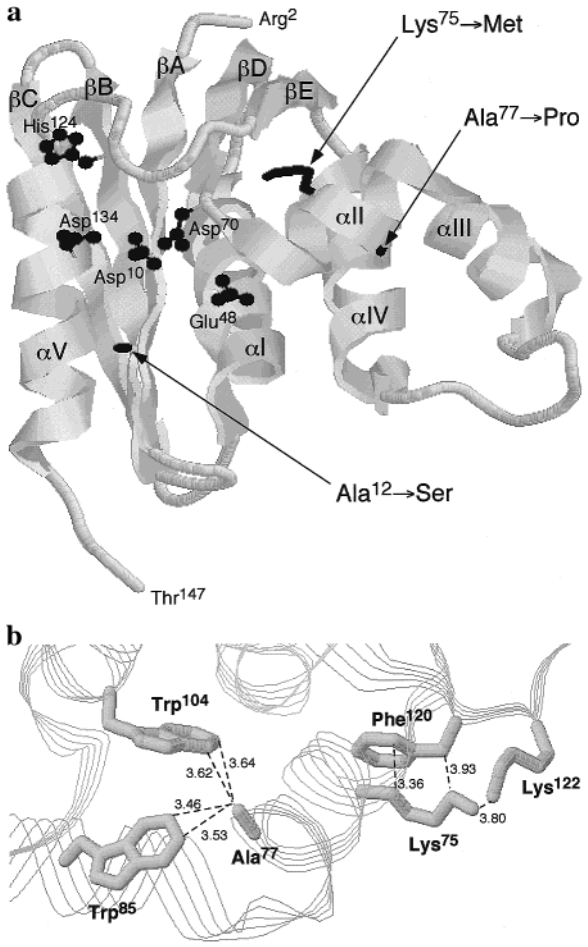

FIGURE 4: Three-dimensional structure of *T. thermophilus* RNase HI. (a) The backbone structure of *T. thermophilus* RNase HI, determined by Ishikawa et al. (*20*), was drawn with the program RasMol. Arg^{2} and Thr^{147} represent the N- and C-terminal residues in this crystal structure, respectively, because the N-terminal region from Met^{-4} to Pro^{1} and the C-terminal region from Pro^{148} to Ala^{161} have not been defined by crystallographic analyses, probably due to structural disorder. The side chains of Ala^{12}, Lys^{75}, and Ala^{77}, as well as the types of amino acid substitutions that enhance the catalytic efficiency of the enzyme, are indicated. In addition, the side chains of the active site residues (Asp^{10}, Glu^{48}, Asp^{70}, His^{124}, and Asp^{134}) are shown. (b) The backbone structure around Lys^{75} and Ala^{77} is shown. The side chains of these residues as well as those of Trp^{85}, Trp^{104}, Phe^{120}, and Lys^{122} are shown. The numbers indicate atomic distances (angstroms). This crystal structure of *T. thermophilus* RNase HI has been deposited in the Brookhaven Protein Data Bank under accession number 1RIL.

stability of the enzyme. In contrast, the $Ala^{77} \rightarrow$ Pro mutation increased both the hydrolysis rate and the affinity of the enzyme for the substrate, but at a cost of protein stability. Neither mutation seriously affected the protein structure. Lys^{75} and Ala^{77}, which correspond to Arg^{75} and Gly^{77} of *E. coli* RNase HI, respectively, are located in the αII helix, which extends from Tyr^{73} to Glu^{80} (Figure 4a). This helix, together with the αI and αIV helices and the βE strand, forms a hydrophobic core of the protein (*20*). In addition, this helix has been proposed to form the substrate binding site (*46*), although none of the specific interactions between this helix and substrate has been identified. Thus, this helix is structurally and functionally important. Nevertheless, six of the eight residues in this helix, which include Leu^{74} and Phe^{78} that form the hydrophobic core, are not conserved in *E. coli* RNase HI. As the result, the αII helix of *T. thermophilus*

RNase HI is shifted away from the molecular center by more than 1 Å as compared to that of *E. coli* RNase HI (*20*). This shift has been suggested to be one of the factors that are responsible for the high stability and low activity of *T. thermophilus* RNase HI at moderate temperatures as compared to those of *E. coli* RNase HI (*20*).

Lys[75] is exposed to the solvent, although the methylene groups in the side chain of this residue seem to make hydrophobic contacts with Phe[120] (Figure 4b). In addition, this amino group probably makes an electrostatic interaction with that of Lys[122] (Figure 4b). Phe[120] and Lys[122] are located in the βE strand (Figure 4a). The loop following this β strand contains His[124]. Because it has been suggested that the flexibility of this loop is important in positioning His[124] to catalyze the hydrolytic reaction (*20*), the Lys[75] → Met mutation may alter the interaction between the βE strand and αII helix and thereby induces a favorable conformational change of His[124]. The Lys[75] → Met mutation did not seriously affect the protein stability, probably because the positive charge repulsion between Lys[75] and Lys[122] does not contribute to protein stability.

Ala[77] is almost fully buried inside the protein molecule. The Ala[77] → Pro mutation destabilized the protein, probably due to the intrinsic destabilization of the αII helix by the introduction of the proline residue. Because this helix is involved in a putative substrate binding site and located close to the active site, a slight conformational change in this helix may induce favorable conformational changes of both the active site and substrate binding site. It has previously been reported that the conformational difference in the αII helix between *T. thermophilus* and *E. coli* RNases HI accounts for a small shift of the side chain of Asp[70] (*20*).

Cooperativity in the Effects of Mutations. The effects of the Lys[75] → Met and Ala[77] → Pro mutations on protein stability, as well as those on protein conformation, are cooperative and not simply independent. These cooperative effects of the mutations are not surprising, because Lys[75] and Ala[77] are located close to each other. The CD spectra shown in Figure 3 suggest that the conformations of the aromatic residues are altered, only when these mutations are simultaneously introduced. In the vicinity of Ala[77], two tryptophan residues (Trp[85] and Trp[104]) are located (Figure 4b). In addition, Tyr[73], Trp[81], and Trp[90] are located around this region. Therefore, it seems likely that the conformation of the αII helix was significantly changed when the Lys[75] → Met and Ala[77] → Pro mutations were simultaneously introduced, and this change forced these aromatic residues to change their configurations. The elimination or introduction of the interactions that specified this conformational change remained to be determined. However, this conformational change is favorable for protein stability, because the K75M/A77P enzyme was more stable than the A77P enzyme by 3.9 °C in T_m and 1.05 kcal/mol in ΔG_m. The effects of the Lys[75] → Met and Ala[77] → Pro mutations on the enzymatic activity were roughly cumulative, indicating that a conformational change caused by the simultaneous introduction of these mutations was not unfavorable for activity as well.

Stability−Activity Relationships. In this study, we showed that the enzymatic activities of *T. thermophilus* RNase HI at both low and high temperatures were improved without a cost of protein stability. This result suggests that hyperthermophilic enzymes are not optimized in their activities even under their physiological conditions. Then the question arises of whether an increase in enzymatic activity of *T. thermophilus* RNase HI is accompanied by an increase in conformational flexibility. We have previously shown that the thermal stability of *E. coli* RNase HI could be improved without serious loss of enzymatic activity (*47*). Hydrogen−deuterium exchange analyses of the *E. coli* RNase HI variant, which is more stable than the wild-type protein by 20.2 °C in T_m, have shown that an increase in stability does not cause global changes in the backbone dynamics on fast and slow time scales (*48*). This result may suggest that proteins are not always stabilized at a cost of conformational flexibility. Hydrogen−deuterium exchange studies can be applied to analyze the conformational flexibility of *T. thermophilus* RNase HI, because the backbone amide hydrogens of this protein have recently been assigned by using heteronuclear NMR spectroscopy (*49*). Therefore, it would be informative to analyze the conformational flexibility of the *T. thermophilus* RNase HI variant with enhanced catalytic efficiency and compare it with that of the wild-type enzyme. These studies will facilitate the understanding of the relationships of stability, activity, and flexibility of enzymes in more detail.

ACKNOWLEDGMENT

We thank ID Biomedical Corp. for providing the 29 b DNA−RNA−DNA for the RNase H assay and Dr. M. Itaya for providing *E. coli* MIC3001.

REFERENCES

1. Kanaya, S., and Itaya, M. (1992) *J. Biol. Chem. 267*, 10184−10192.
2. Wrba, A., Schweiger, A., Schultes, V., and Jaenicke, R. (1990) *Biochemistry 29*, 7584−7592.
3. Varley, P. G., and Pain, R. H. (1991) *J. Mol. Biol. 220*, 531−538.
4. Zavodszky, P., Kardos, J., Svingor, A., and Petsko, G. A. (1998) *Proc. Natl. Acad. Sci. U.S.A. 95*, 7406−7411.
5. Kohen, A., Cannio, R., Bartolucci, S., and Klinman, J. P. (1999) *Nature 399*, 496−499.
6. Meiering, E. M., Serrano, L., and Fersht, A. R. (1992) *J. Mol. Biol. 225*, 585−589.
7. Shoichet, B. K., Baase, W. A., Kuroki, R., and Matthews, B. W. (1995) *Proc. Natl. Acad. Sci. U.S.A. 92*, 452−456.
8. Kidokoro, S., Miki, Y., Endo, K., Wada, A., Nagao, H., Miyake, T., Aoyama, A., Yoneya, T., Kai, K., and Ooe, S. (1995) *FEBS Lett. 367*, 73−76.
9. Giver, L., Gershenson, A., Freskgard, P. O., and Arnold, F. H. (1998) *Proc. Natl. Acad. Sci. U.S.A. 95*, 12809−12813.
10. Chen, K., and Arnold, F. H. (1993) *Proc. Natl. Acad. Sci. U.S.A. 90*, 5618−5622.
11. Wan, L., Twitchett, M. B., Eltis, L. D., Mauk, A. G., and Smith, M. (1998) *Proc. Natl. Acad. Sci. U.S.A. 95*, 12825−12831.
12. Zhao, H., and Arnold, F. H. (1999) *Protein Eng. 12*, 47−53.
13. Matsuura, T., Miyai, K., Trakulnaleamsai, S., Yomo, T., Shima, Y., Miki, S., Yamamoto, K., and Urabe, I. (1999) *Nat. Biotechnol. 17*, 58−61.
14. Merz, A., Yee, M. C., Szadkowski, H., Pappenberqer, G., Crameri, A., Stemmer, W. P. C., Yanofsky, C., and Kirschner, K. (2000) *Biochemistry 39*, 880−889.
15. Itaya, M., and Kondo, K. (1991) *Nucleic Acids Res. 19*, 4443−4449.
16. Ohtani, N., Haruki, M., Morikawa, M., and Kanaya, S. (1999) *J. Biosci. Bioeng. 88*, 12−19.
17. Crouch, R. J. (1990) *New Biol. 2*, 771−777.

18. Hostomsky, Z., Hostomska, Z., and Matthews, D. A. (1993) in *Nucleases* (Linn, S. M., and Roberts, R. J., Eds.) 2nd ed., pp 341−376, Cold Spring Harbor Laboratory Press, Cold Spring Harbor, NY.
19. Kanaya, S. (1998) in *Ribonucleases H* (Crouch, R. J., and Toulme, J. J., Eds.) pp 1−38, INSERM, Paris.
20. Ishikawa, K., Okumura, M., Katayanagi, K., Kimura, S., Kanaya, S., Nakamura, H., and Morikawa, K. (1993) *J. Mol. Biol. 230*, 529−542.
21. Katayanagi, K., Miyagawa, M., Matsushima, M., Ishikawa, M., Kanaya, S., Ikehara, M., Matsuzaki, T., and Morikawa, K. (1990) *Nature 347*, 306−309.
22. Katayanagi, K., Miyagawa, M., Matsushima, M., Ishikawa, M., Kanaya, S., Nakamura, H., Ikehara, M., Matsuzaki, T., and Morikawa, K. (1992) *J. Mol. Biol. 223*, 1029−1052.
23. Yang, W., Hendrickson, W. A., Crouch, R. J., and Satow, Y. (1990) *Science 249*, 1398−1405.
24. Itaya, M., and Crouch, R. J. (1991) *Mol. Gen. Genet. 227*, 424−432.
25. Itaya, M., McKelvin, D., Chatterjie, S. K., and Crouch, R. J. (1991) *Mol. Gen. Genet. 227*, 438−445.
26. Campbell, A. G., and Ray, D. S. (1993) *Proc. Natl. Acad. Sci. U.S.A. 90*, 9350−9354.
27. Hesslein, D. G. T., and Campbell, A. G. (1997) *Mol. Biochem. Parasitol. 86*, 121−126.
28. Itaya, M. (1990) *Proc. Natl. Acad. Sci. U.S.A. 87*, 8587−8591.
29. Zhang, Y.-B., Ayalew, S., and Lacks, S. A. (1997) *J. Bacteriol. 179*, 3828−3836.
30. Haruki, M., Hayashi, K., Kochi, T., Muroya, A., Koga, Y., Morikawa, M., Imanaka, T., and Kanaya, S. (1998) *J. Bacteriol. 180*, 6207−6214.
31. Haruki, M., Noguchi, E., Akasako, A., Oobatake, M., Itaya, M., and Kanaya, S. (1994) *J. Biol. Chem. 269*, 26904−26911.
32. Kanaya, S., Kohara, A., Miyagawa, M., Matsuzaki, T., Morikawa, K., and Ikehara, M. (1989) *J. Biol. Chem. 264*, 11546−11549.
33. Miller, J. H. (1972) in *Experiments in Molecular Genetics* (Miller, J. H., Ed.) pp 433, Cold Spring Harbor Laboratory Press, Cold Spring Harbor, NY.
34. Kanaya, S., Oobatake, M., Nakamura, H., and Ikehara, M. (1993) *J. Biotechnol. 28*, 117−136.
35. Sanger, F., Nicklen, S., and Coulson, A. R. (1977) *Proc. Natl. Acad. Sci. U.S.A. 74*, 5463−5467.
36. Stemmer, W. P. C. (1994) *Nature 370*, 389−390.
37. Haruki, M., Noguchi, E., Nakai, C., Liu, Y.-Y., Oobatake, M., Itaya, M., and Kanaya, S. (1994) *Eur. J. Biochem. 220*, 623−631.
38. Dower, W. J., Miller, J. H., and Ragsdale, C. W. (1988) *Nucleic Acids Res. 16*, 6127−6145.
39. Hirano, N., Haruki, M., Morikawa, M., and Kanaya, S. (1998) *Biochemistry 37*, 12640−12648.
40. Laemmli, U. K. (1970) *Nature 227*, 680−685.
41. Kimura, S., Nakamura, H., Hashimoto, T., Oobatake, M., and Kanaya, S. (1992) *J. Biol. Chem. 267*, 21535−21542.
42. Becktel, W. J., and Schellman, J. A. (1987) *Biopolymers 26*, 1859−1877.
43. Kanaya, S., Kohara, A., Miura, Y., Sekiguchi, A., Iwai, S., Inoue, H., Ohtsuka, E., and Ikehara, M. (1990) *J. Biol. Chem. 265*, 4615−4621.
44. Green, N. M., and Melamed, M. D. (1966) *Biochem. J. 100*, 614−621.
45. Kanaya, S., Oobatake, M., and Liu, Y.-Y. (1996) *J. Biol. Chem. 271*, 32729−32736.
46. Nakamura, H., Oda, Y., Iwai, S., Inoue, H., Ohtsuka, E., Kanaya, S., Kimura, S., Katsuda, C., Katayanagi, K., Morikawa, K., Miyashiro, H., and Ikehara, M. (1991) *Proc. Natl. Acad. Sci. U.S.A. 88*, 11535−11539.
47. Akasako, A., Haruki, M., Oobatake, M., and Kanaya, S. (1995) *Biochemistry 34*, 8115−8122.
48. Yamasaki, K., Akasako-Furukawa, A., and Kanaya, S. (1998) *J. Mol. Biol. 277*, 707−722.
49. Hollien, J., and Marqusee, S. (1999) *Proc. Natl. Acad. Sci. U.S.A. 96*, 13674−13678.

BI0015008